Apparent intensity dependence of shunts in PV modules Revision of the shunt parameterization in the De Soto Model and PVsyst

Nils-Peter Harder[1] and José Cano Garcia[1]

[1]TotalEnergies

August 27, 2024

Abstract

It is common practice in PV system simulation to use the De Soto model, which describes how to use the 1-diode equivalent circuit model for modules. De Soto's model scales the shunt with irradiance, making it disappear towards zero W/m ^{2}. Also, the commercial software PVsyst uses a parameterization that reduces the shunt effect when the irradiance goes down. However, the Si solar cells that make up a module typically do not have an illumination dependent shunt. We therefore investigate the origin of the intensity dependent apparent shunt in modules. We show that this apparent shunt (derived from the slope of the quasi-linear region from I_{SC} onwards) is a misinterpretation and has little to do with a shunt conductance. Instead, the module I- V curve slope of the quasi-linear region from I_{SC} onwards stems from I_{SC} mismatches between the cells. Such mismatch can occur from small illumination inhomogeneity or cell production variation. Abandoning the practice of using the I- V curve slope to determine the shunt value for equivalent circuit models of modules (and the corresponding shunt scaling in the De Soto model or PVsyst), contributes to physically more meaningful I- V curve parameterizations and possibly also more accurate PV system energy yield prediction.

ABSTRACT: It is common practice in PV system simulation to use the De Soto model, which describes how to use the 1-diode equivalent circuit model for modules. De Soto's model scales the shunt with irradiance, making it disappear towards zero W/m^2. Also, the commercial software PVsyst uses a parameterization that reduces the shunt effect when the irradiance goes down. However, the Si solar cells that make up a module typically do not have an illumination dependent shunt. We therefore investigate the origin of the intensity dependent apparent shunt in modules. We show that this apparent shunt (derived from the slope of the quasi-linear region from I_{SC} onwards) is a misinterpretation and has little to do with a shunt conductance. Instead, the module I-V curve slope of the quasi-linear region from I_{SC} onwards stems fromI_{SC} mismatches between the cells. Such mismatch can occur from small illumination inhomogeneity or cell production variation. Abandoning the practice of using the I-V curve slope to determine the shunt value for equivalent circuit models of modules (and the corresponding shunt scaling in the De Soto model or PVsyst), contributes to physically more meaningful I-Vcurve parameterizations and possibly also more accurate PV system energy yield prediction.

Keywords: Module performance, I -V curve parameterization, Shunt characterization.

1 INTRODUCTION

For single solar cells, the slope at I_{SC} [or rather: the slope between I_{SC} and some mid-sized voltage well before the maximum power point (MPP) where the recombination current is still very small] can be interpreted as shunt conductance [?]I / [?]V = 1 / R_{Sh}. For single cells, this shunt value can be used for equivalent circuit models of such single cells, for example in a 1-diode or 2-diode model. We call this quantity $R_{Sh.Slope}$, as it is derived from the I -V curve slope between I_{SC} and some mid-sized voltages before the curvature of the exponential term becomes notable. By applying this type of analysis, De Soto et

al. [1] and Mermoud et al. [2], for example, observed that module $I!V$ curves have an intensity-dependent $R_{\text{Sh.Slope}}$. De Soto et al. and Mermoud et al. interpreted this slope as the shunt conductance and also provided parameterizations of this slope as a function of illumination intensity for their 1-diode model parameterization of modules. An intensity dependent shunt in modules is surprising, or possibly even implausible, because on cell level there is typically no indication that an equivalent-circuit model would need an intensity-dependent shunt for describing the maximum power point (MPP) of a solar cell, not even for describing the MPP for a very wide range of intensities [3]. (Note that the academically interesting and very small effect of a seemingly intensity-dependent shunt, as described by Robinson [4], and later explained by Breitenstein [5], is an effect of light I - V curves that vanishes well before the MPP. This effect, that we call "photoshunt", is therefore of no relevance for an equivalent circuit model that seeks to describe the power production of a cell or module.)

We show in this paper the origin of the intensity dependence of $R_{\text{Sh.Slope}}$. For modules, this slope-derived $R_{\text{Sh.Slope}}$ is not related to an actual shunt conductance, and instead it is the result of I_{SC}-mismatches between the cells, combined with their reverse-bias characteristics. Note that such I_{SC} mismatch might stem from an illumination inhomogeneity in a module measurement [6], from variations in cell manufacturing, or a combination of these two effects.

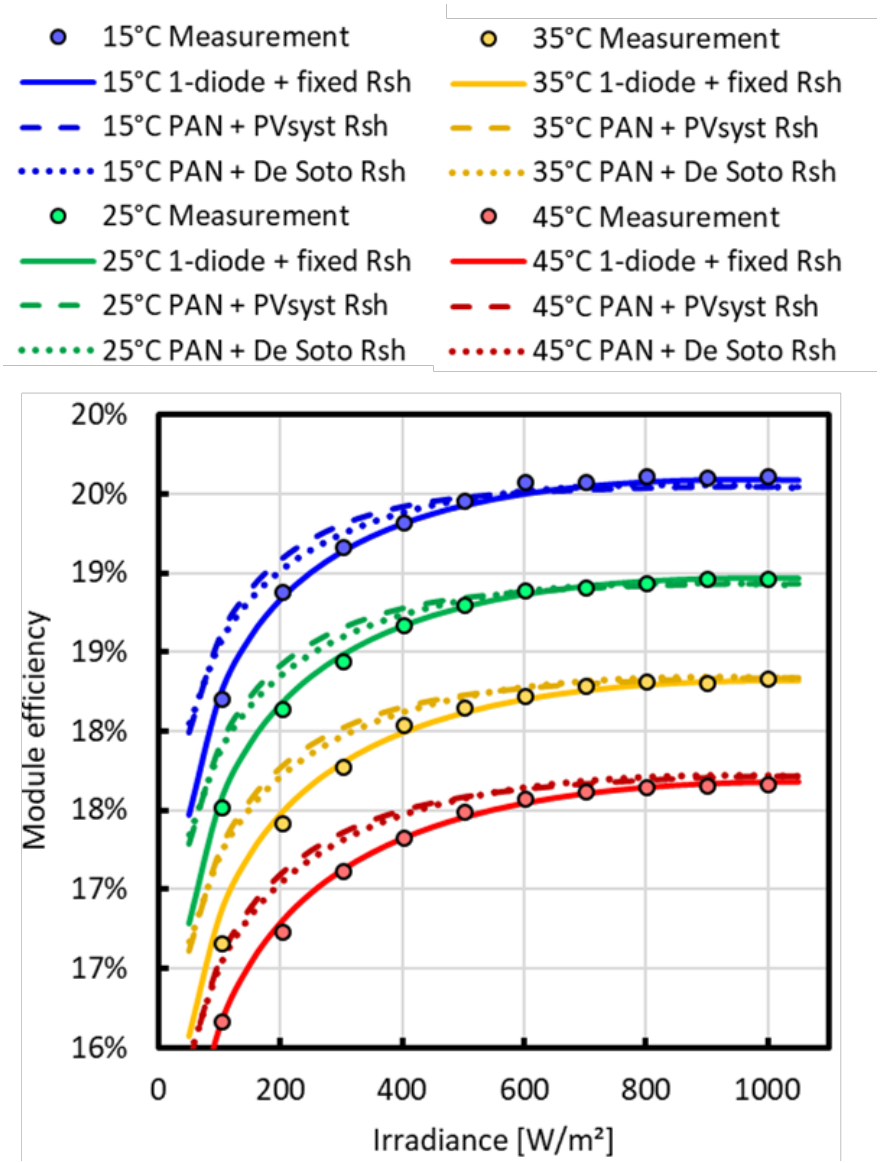

Figure 1: Measured efficiencies of a TOPCon module (symbols) and calculated efficiencies by the 1-diode model (solid lines), with a fixed shunt R_{Sh}, and using a simple series resistance R_S, independent of temperature and intensity, from reference [7]. The dashed and dotted lines are calculated efficiencies based on PVsyst's [2] (dashed lines), or De Soto's [1] (dotted lines) approach, which both use an intensity dependent shunt.

Importantly, and as has been discussed already in our recent module characterization study [7], using $R_{Sh.Slope}$ as shunt resistance in an equivalent circuit model for the I - V curve of modules leads to physical inconsistencies: $R_{Sh.Slope}$ typically has a rather low value, but (as this present paper will show in detail) does not represent an actual shunt conductance. Using this value $R_{Sh.Slope}$ nevertheless for the shunt in equivalent circuit models (e.g. a 1-diode model) and trying to reproduce V_{OC} and MPP values, leads to needing to use a too low ideality factor value for the module I - V curve. In our recent characterization study of a TOPCon module [7] we found exactly such phenomenon: PAN file specified low shunt values that correspond to the measured $R_{Sh.slope}$, in combination with an implausibly low ideality factor in the PAN

file. Note that a wrong (too low) ideality factor in turn, affects the temperature-dependency of the modeled module performance. As a consequence, the simulation software PVsyst introduces without physical basis a temperature dependency for the ideality factor (by using a temperature coefficient "muGamma").

It shall be pointed out that a simple model, that neither uses the complication of an intensity-dependent shunt nor an unphysical feature such as a temperature dependent ideality factor, is not only advantageous by virtue of its simplicity and better physical interpretability. As is shown here in Fig. 1, taken from reference [7], such simpler model also leads to accurate (and seemingly even more accurate) module performance parameterization over a wide range of illumination intensities and temperatures.

We set out in this paper to explore the origin of the intensity dependent I -V curve slope from I_{SC}onwards (i.e. the intensity dependent $R_{\mathrm{Sh.Slope}}$) by using a simple 1-diode model for the individual cells, connected in series to a 60-cell module. This simple model obviously (and deliberately) does not contain the effects of the apparent shunt discovered by Robinson [4] and explained by Breitenstein [5]. We make this choice for two reasons:

Firstly, Robinson's "photoshunt" is very small and affects in no conditions known to us the MPP. In consequence, it is typically not considered at all in equivalent circuit models that seek to describe power production by solar cells [3]. It is nevertheless fair to say that to some small degree Robinson's photoshunt will have some contribution to the appearance of an illumination intensity dependence of the module I -V curve slope in the quasi-linear region from I_{SC} onwards. However, we deem this contribution to be marginal in practice for PV modules.

Secondly, and more importantly, by focusing on a simple model, we can highlight in a very pointed manner the main origin of the intensity-dependent $R_{\mathrm{Sh.Slope}}$. In this way we can show how by combining individual cells that each do not feature an intensity dependent shunt, the phenomenon of an intensity dependent apparent shunt $R_{\mathrm{Sh.Slope}}$ emerges in a module.

2 MODEL DESCRIPTION

We represent individual solar cells by the "1-Diode model" equivalent circuit model, shown in Fig. 2. The I -V curve of the 1-Diode model is given in equation 1:

$$\begin{aligned} I[V] = \quad & I_{\mathrm{PH}}[\Phi] \\ & - I_0 \times \left(\mathrm{Exp}\left[\frac{q(V+I[V]\times R_S)}{n \times kT}\right] - 1\right) \\ & - \frac{V+I[V]\times R_S}{R_{\mathrm{Sh}}} \end{aligned} \tag{1}$$

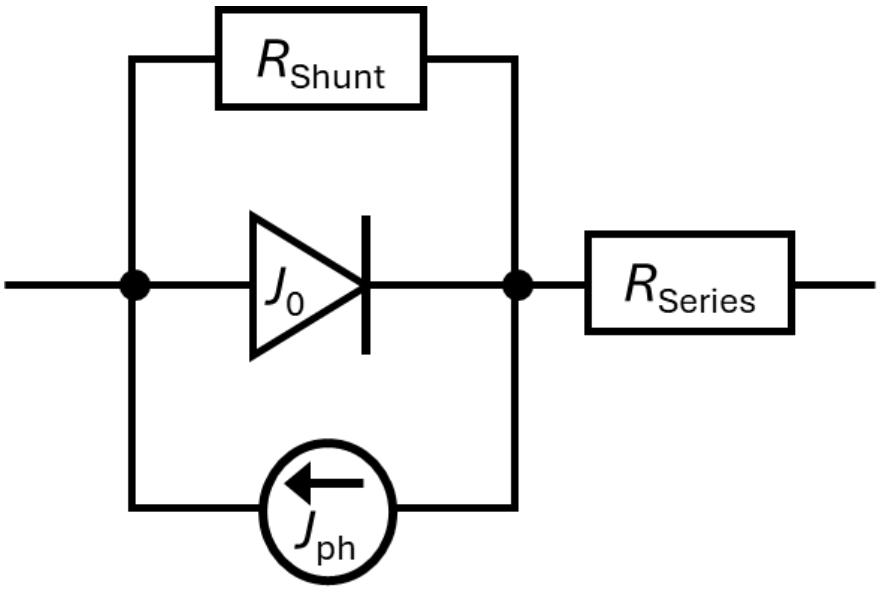

Figure 2: 1-Diode model used in this paper for representing one individual cell in the module circuit.

$I_{PH}(\varphi)$ is the photogeneration of current in the solar cell, which is directly proportional to the illumination intensity φ. In the typical parameter range of well-working silicon solar cells,$I_{PH}(\varphi)$ is numerically almost identical to the short-circuit current I_{SC} at illumination intensity φ. The variable I_0 is the saturation current density, R_S is the series resistance,R_{Sh} the shunt resistance, V is the voltage at the terminals of the solar cell, q the elemental charge,kT is the product of the Boltzmann constant k and the temperature T . The ideality factor is specified by the variable$n$. Except for the photogenerated current$I_{PH}(\varphi)$, all variables are independent of the illumination intensity φ. The illumination intensity (or irradiance) φ is typically given in W/m^2, where the standard test condition (STC) corresponds to 1000 W/m^2 with an AM1.5G spectrum. We will refer to this standard intensity in this paper as "1 Sun", and 0.5 Sun or 0.2 Sun refer therefore to 500 W/m^2 and 200 W/m^2, respectively.

Unless otherwise stated, the standard parameter set for the area-specific values of the parameters in equation 1 are those listed in Table I.

Table I: Standard set of parameter values of the 1-Diode parameterization used in this study

$I_{PH}[\varphi]$	R_S	R_{Sh}	I_0	n
40 mA/cm^2 per Sun	0.5 cm^2	10 kcm^2	58.7 fA/cm^2	1

Fig. 3 shows a schematic of the module structure in this study. The bypass diodes are modeled with an ideality factor $n = 1$, letting our standard cell I_{SC} pass at 0.2 V.

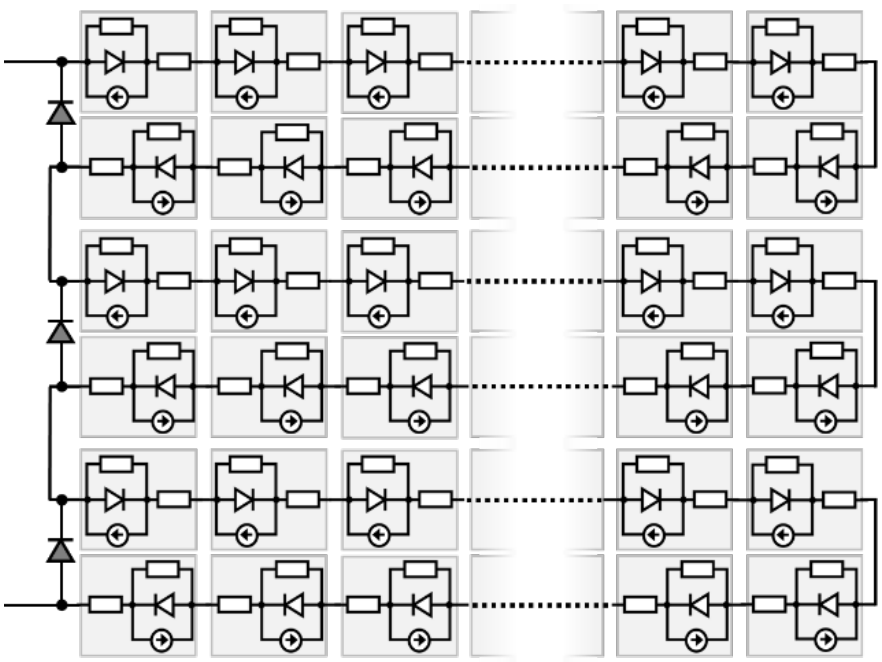

Figure 3: Equivalent circuit for representing a 60-cell module. Each individual cell in this circuit is represented by the1-Diode model shown in Fig. 2. The diode symbols in grey on the left represent bypass diodes.

For our study of the effect of I_{SC} mismatches between the individual cells of the module, we make use of an illumination inhomogeneity map published by Ramspeck [6], describing the cetisPV-Moduletest4 system of halm elektronik GmbH. The 270 cm x 160 cm illumination area of this module tester has an inhomogeneity of +/- 0.4%. Fig. 4 shows a center section of 6 x 10 cell positions of the illumination intensity map published by Ramspeck.

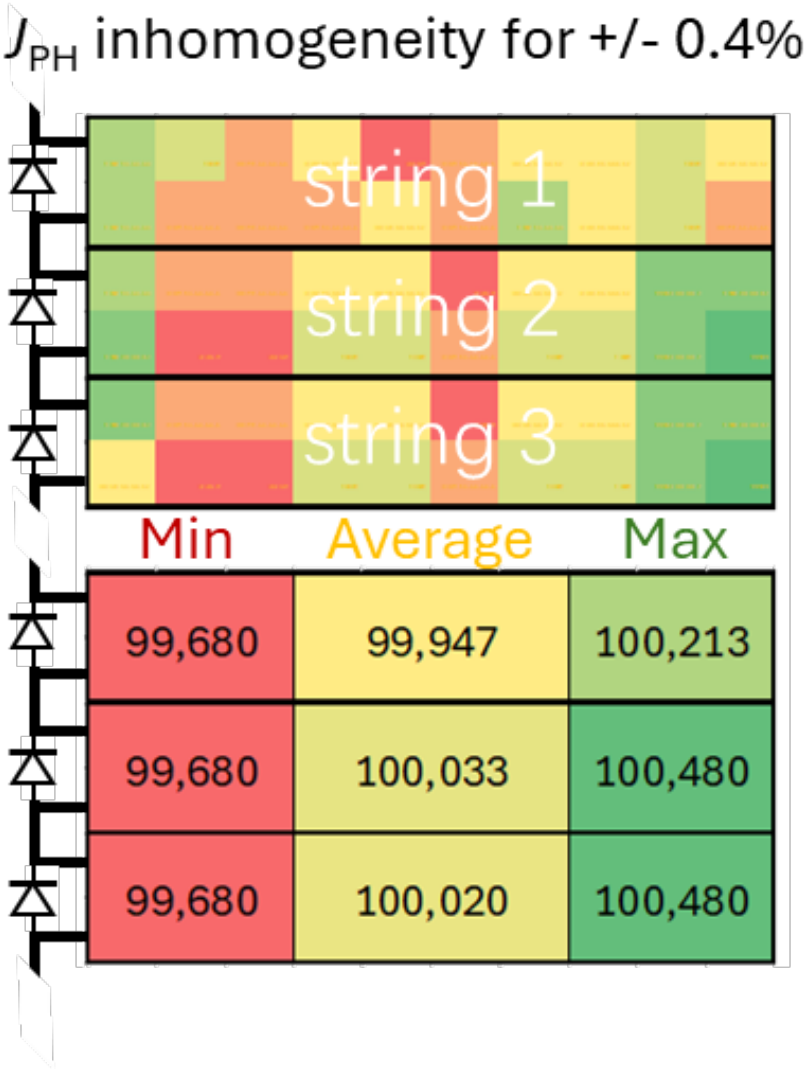

Figure 4: Inhomogeneity map [in "% of average"] of the photogeneration J_{PH} used for the simulation of modules with I_{SC}-mismatched cells. The 6 x 10 distribution in the upper schematic is taken from a subset of the intensity data map of the paper of Ramspeck [6]. The lower schematic lists minimum, average and maximum photogeneration in the cells of the three different cell strings in the module, and it additionally serves as color scale for upper schematic with the +/- 0.4% inhomogeneity case shown here.

In case of completely identical cells in the module, the illumination intensity map in Fig. 4 translates directly into an identicalI_{PH} photogeneration map. It therefore describes the best expectable I_{SC} inhomogeneity distribution, limited only by the illumination inhomogeneity of a state-of-the-art module flash tester.

We will also explore the effect of larger inhomogeneities, by usingI_{PH} maps that are scaled from the +/- 0.4% inhomogeneous map of Fig. 4 to inhomogeneities of +/- 1.0% and +/- 2.0%. These larger inhomogeneities can be understood as either representing measurements with a less ideal module flash tester, or representing I_{PH} inhomogeneity distributions originating from a combination of cell production quality variation in with an illumination area inhomogeneity.

Note that our inhomogeneity map consists of only seven different values, as is shown in the histogram in

Fig. 5 for the +/- 0.4% inhomogeneity case. Our cases of increased inhomogeneity only spread these seven values over a larger minimum-to-maximum range. These maps are therefore only a rough representation of a real-world inhomogeneity distribution but will serve sufficiently well to show the fundamental effects of inhomogeneity.

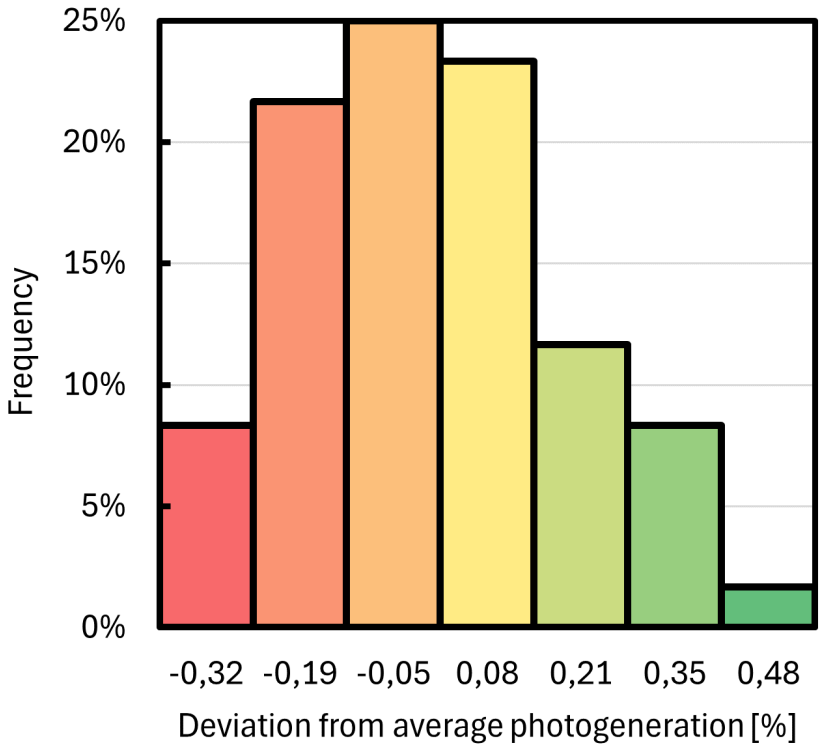

Figure 5: Histogram of the deviation from the average photogeneration in the inhomogeneity map shown in Fig.4 (+/- 0.4% inhomogeneity case). In our data set, the photogeneration deviations for each category are a single value (the value shown on the horizontal axis), and not a continuous spread.

It can be seen from Fig. 4 that the average values, and also the minimum and maximum values of the three strings, are very similar. It can therefore be expected that the bypass diodes will have only a minor effect on the I -V curves, which is also what we found in our simulations. However, in an inhomogeneity scenario, individual cells will be forced into reverse bias along the lower voltage range of the$I$ -V curves, also in the presence of bypass diodes. We therefore have to consider the reverse-bias characteristics of the individual cells when exploring the effects ofI_{PH} inhomogeneity.

Clement *et al* . [8] published reverse-bias characteristics for different solar cell technologies, and Fig. 6 shows as curve in red (case 1, labelled "IBC homojunction") a digitized version of the reverse bias characteristics published by Clement *et al* . for IBC cells.

Case 3, the black curve in Fig. 4 is the simplest case, using for forward and reverse characteristics the sameR_{Shunt} resistance (see also Table I with the standard parameter set used in this study).

The blue curve, i.e. case 2, uses also the sameR_{Shunt} in forward and reverse characteristics, but in combination with an added "softened break-through" compared to the "IBC homojunction" of case 1. This break-through

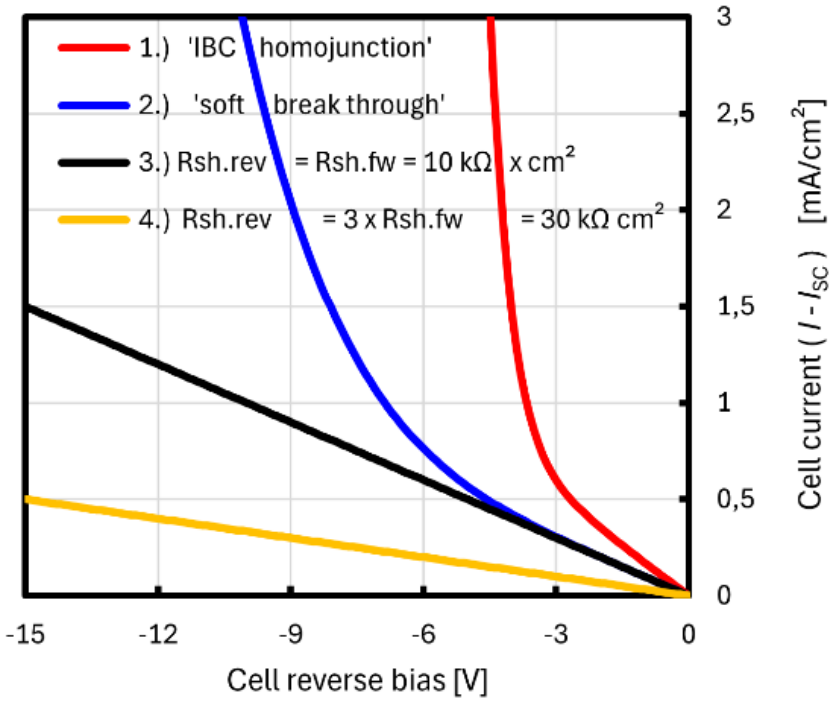

Figure 6: Reverse-characteristics of cell I -V curves used in the simulations in this paper for modules with I_{SC}-mismatched cells.

characteristics of the case 2 blue curve is approximately identical to a 3-fold increase of the reverse breakthrough reported by Clement *et al.* [8] for PERC solar cells under 1-Sun illumination intensity.

The yellow curve in Fig. 6, i.e. case 4, uses in reverse direction a three-times higher shunt resistance than in forward direction. Neither cases 3 nor 4 feature a reverse breakthrough and have only a linear reverse-bias characteristics. While a real solar cell does have a break-through at some reverse-bias voltage, these purely linear reverse bias cases can be regarded as cases representing cells with a very high break-through voltage.

3 RESULTS

3.1 I_{SC}-matched cells

For a scenario of I_{SC} matched cells we have to consider only the parameters I_0, n ,R_{Sh} and R_S, because I_{PH} is virtually identical to I_{SC} for all practical scenarios that we need to consider here. Variations of the series resistance R_S amongst the cells do not cause effects that would be misinterpreted as an intensity dependent shunt. This can be easily understood by noting that the individual series connected elements of the string circuits in Fig. 3 can be regrouped, such that all series resistances of the individual cells are placed on one end of the re-grouped string circuit, and all diode-containing elements on the other end. In other words, all series resistances can be lumped together into one big resistance, and its effect does not depend on the distribution of individual cell R_S values that the lumped big series resistance originated from.

It is therefore of bigger interest to examine what effect have distributions of I_0 values, ideality factor values n , and distributions of shunt values R_{Sh}.

In a voltage range where the exponential part of equation 1 dominates the current for all cells, we can approximate and re-write equation 1 for all cells as:

$$V = n\frac{\mathrm{kT}}{q} \times Ln\left[\frac{I(V)-I_{\mathrm{PH}}}{I_0}\right] - I\,(V) \times R_S \quad (2)$$

$I\ (V\ )$ is identical for all cells, and so is$I\ _{\mathrm{PH}}$, because we considered only the case of$I\ _{\mathrm{SC}}$-matched cells. It therefore follows for the module voltage $V\ _{\mathrm{M}}$:

$$\mathrm{V}_M = \mathrm{kT}\frac{}{q\left(\mathrm{Ln}[I(V)-I_{\mathrm{PH}}]\sum_{i=1}^{N} n_i - \sum_{i=1}^{N} n_i\ \mathrm{Ln}[I_{0,i}]\right)}\text{-}\mathrm{I}(V) \times R_L \quad (3)$$

. . . where N is the number of cells in series,$R\ _{\mathrm{L}}$ is the sum of all cell series resistances$R\ _{\mathrm{S,i}}$, and the index "i " in equation 3 refers the i -th cell. With the definition of$n\ _{\mathrm{av}}$ as the arithmetic average of all ideality factors $n\ _{\mathrm{i}}$, we find:

$$q\frac{V_M + I(V)\times R_L}{\mathrm{kT}\ \ n_{\mathrm{av}}\ \ \mathrm{N}} = Ln\left[\frac{I(V)-I_{\mathrm{PH}}}{\prod_{i=1}^{N} I_{0,i}^{\ \frac{n_i}{n_{\mathrm{av}}\ \mathrm{N}}}}\right] \quad (4)$$

. . . which is essentially the 1-Diode equation for a module without shunt, as can be seen by rewriting it as:

$$\mathrm{I}(V) = \mathrm{I_{PH}} - \ I_{0,M}\left(\mathrm{Exp}\left[\frac{q(V_M + I(V)\times R_L)}{N\ \times\ n_{\mathrm{av}}\ \times kT}\right] - 1\right) \quad (5)$$

. . . where$I_{0,M} = \ \prod_{i=1}^{N} I_{0,i}^{\ \frac{n_i}{n_{\mathrm{av}}\ \mathrm{N}}}$, and we added the "-1" of equation 1 that we dropped in equations 2 to 4. We therefore can conclude that no mix of ideality factors$n\ _{\mathrm{i}}$ and saturation currents$I\ _{\mathrm{0,i}}$ will create the emergence of a term that appears like a shunt, nor as an intensity dependent shunt.

Similarly one can show for the voltage range where the exponential part of equation 1 does not dominate for any of the cells (and thus only their linear shunt terms dominate the current) that the module$I$ -V curve is described by a shunt term that stems from the sum of all individual shunts $R\ _{\mathrm{Sh,i}}$:

$$I\,(V) = I_{\mathrm{PH}} - \frac{V_M + I(V)\times R_L}{\sum_{i=1}^{N} R_{Sh,i}} \quad (6)$$

For $I\ _{\mathrm{SC}}$ matched cells it therefore remains to consider voltage ranges where the exponential of some cells and the linear shunt term of other cells of equation 1 are relevant for the module current. To verify whether such combination can lead to$I$ -V curve shapes that could be interpreted as intensity dependent shunts, we plot in Fig. 7 the I -V curves of modules with different shunt value distributions across the cells in the module. The colored curves in Fig. 7 represent module circuits where different amounts of the cells in the module have a notably lower shunt resistance of 120 $\mathrm{cm}^{\mathbf{2}}$ than the rest of the cells with a 10 kcm2 shunt of the standard set of 1-Diode cell model parameters in Table I. The dashed lines represent modules with identical cells, each of them described by the parameter set of Table I. The solid black lines represent a linear variation of the of shunt conductance $1/\mathrm{R_{Sh}}$ across the individual cells in the circuit.

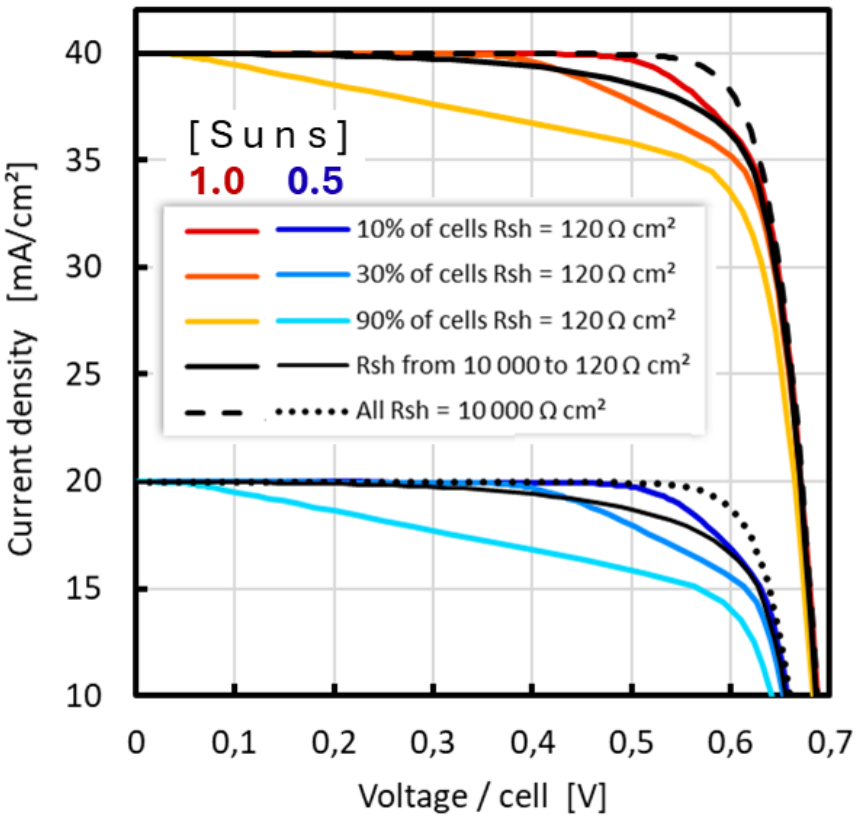

Figure 7: I -V curves at 1 Sun (upper range of curves) and 0.5 Sun (lower range of curves), plotted for I_{SC}-matched cells in the module circuit shown in Fig. 3, with different assumptions for the R_{Shunt} distribution amongst the individual cells.

We can see in Fig. 7 that inhomogeneous shunt distributions across the different cells in the module circuit all produce I -V curve shapes that clearly cannot be described by a simple shunt model. No single value of a voltage-independent effective shunt can produce such I -V curve shapes. However, apart from a minor series resistance effect, the slopes of the curves are identical when comparing 1 Sun to 0.5 Sun curves. We can therefore conclude that also shunt distributions cannot create I -V curve shapes that could be interpreted as some kind of illumination dependent shunt resistance.

3.1 Modules with I_{SC} mismatched cells

In this section we show simulation results for modules where each individual cell is described by the standard model parameters of Table I, except for a variation of the photogeneration current I_{PH}. The photogeneration current distribution amongst the cells is according to the inhomogeneity map shown in Fig. 4. We scale the inhomogeneity distribution of this map to three different levels of maximum-to-minimum variations: +/- 0.4%, +/- 1.0%, and +/- 2.0%. Since photogeneration current inhomogeneities amongst the cells will drive some cells into reverse bias, we explore the effect of the four different reverse bias characteristics shown in Fig. 6.

Fig. 8 shows four plots, each representing a module where all cells in the module have one of the four different reverse bias characteristics of Fig. 6. In each plot there are different curves that correspond to different degrees of inhomgeneities of the photogeneration across the cells in the module circuit: +/- 0.4%, +/- 1.0%, and +/- 2.0%. The quantity plotted in these graphs is the slope of the simulated I -V curves between I_{SC}

and 450 mV/cell. (Very similar results are obtained for other choices, such as the slope between I_{SC} and 300 mV/cell.) The inverse of these slopes is the apparent shunt resistance $R_{Sh.Slope}$. The horizontal axis of the graphs in Fig. 8 is the illumination intensity expressed in Suns (1 Sun = 1000 W/m²).

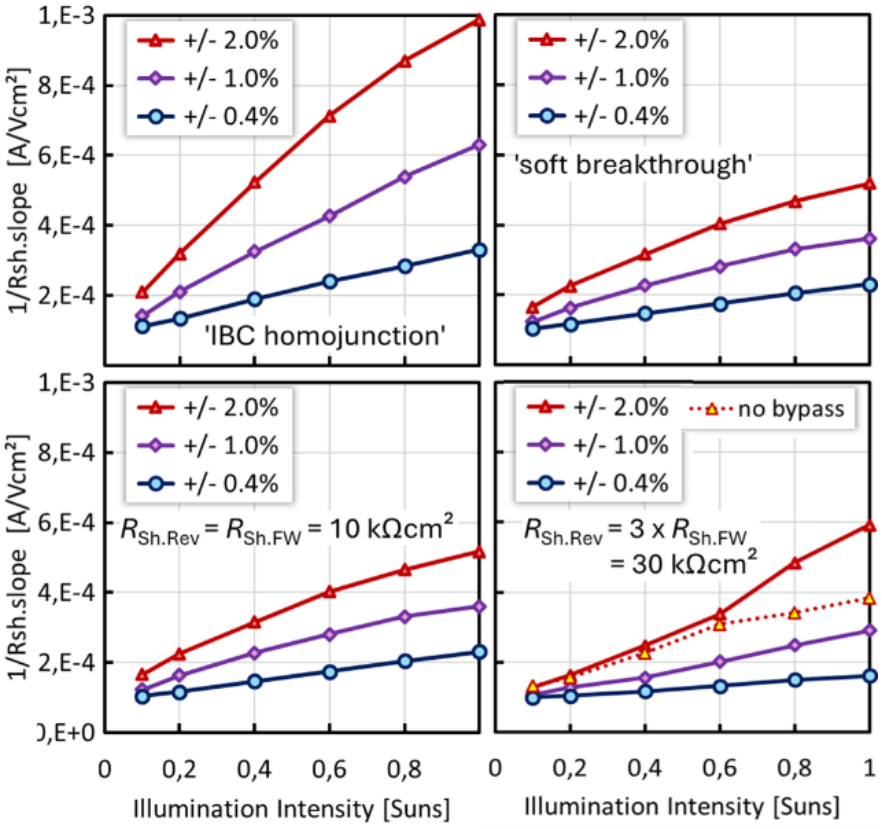

Figure 8: Inverse apparent shunt resistances $R_{Sh.Slope}$ derived from the I -V -curve slopes between I_{SC} and 450 mV/cell, plotted as a function of illumination intensity in Suns. Each graph represents one type of reverse bias characteristics (see Fig. 6), and each curve refers to one photogeneration inhomogeneity distribution +/- 0.4%, +/- 1.0%, and +/- 2.0%.

The lower right graph in Fig. 8 features an additional fourth curve with a dotted red line, showing for the case of +/- 2% photogeneration inhomogeneity the difference between a module circuit with and without bypass diodes. In the other cases of this study, the difference due to the bypass diodes is small and is therefore not shown explicitly here.

We can clearly see in Fig. 8 that cell photogeneration inhomogeneities of the cells in the module circuit cause the emergence of an intensity dependent apparent shunt $R_{Sh.Slope}$, even though all individual cells have an identical and intensity independent shunt. The magnitude of the apparent shunt $R_{Sh.Slope}$ does not only depend on the illumination intensity and inhomogeneity, but also on the cells' reverse bias characteristics. Generally, the more efficiently the cells are able to conduct current in reverse bias direction, the more pronounced is the illumination intensity dependence of the apparent shunt conductance $1/R_{Sh.Slope}$. Note that towards zero illumination intensity the value of $1/R_{Sh.Slope}$ converges towards the value of 1×10^{-4} 1/(cm²). This value corresponds to the forward-bias shunt value of 10 kcm2 that all cells in these simulations share (see also Table I).

Fig. 9 provides a closer look at simulated module I -V curves for the case of +/- 2.0% inhomogeneity of the photogeneration I_{PH} of the cells in the module circuit. Note that all four module I -V curves were generated

with a set of cell definitions that have completely identical forward-bias characteristics. Nevertheless, the forward characteristics of the module I -V curves are different for a wide range of forward voltages up to close to the maximum power voltage V_{MP} at the MPP. Very unlike a real shunt, this effect ends in a sharp kink as all I -V curves merge rather abruptly into the grey dotted I -V curve, representing a module with homogeneous I_{PH} for the cells.

Note that despite clearly visible I -V curve differences in Fig. 9, the four curves agree perfectly well with each other in the voltage range of the MPP. Thus, despite different $R_{\mathrm{Sh.Slope}}$ values, the maximum power production of these four different modules is identical and unaffected by different values of the apparent shunt $R_{\mathrm{Sh.Slope}}$.

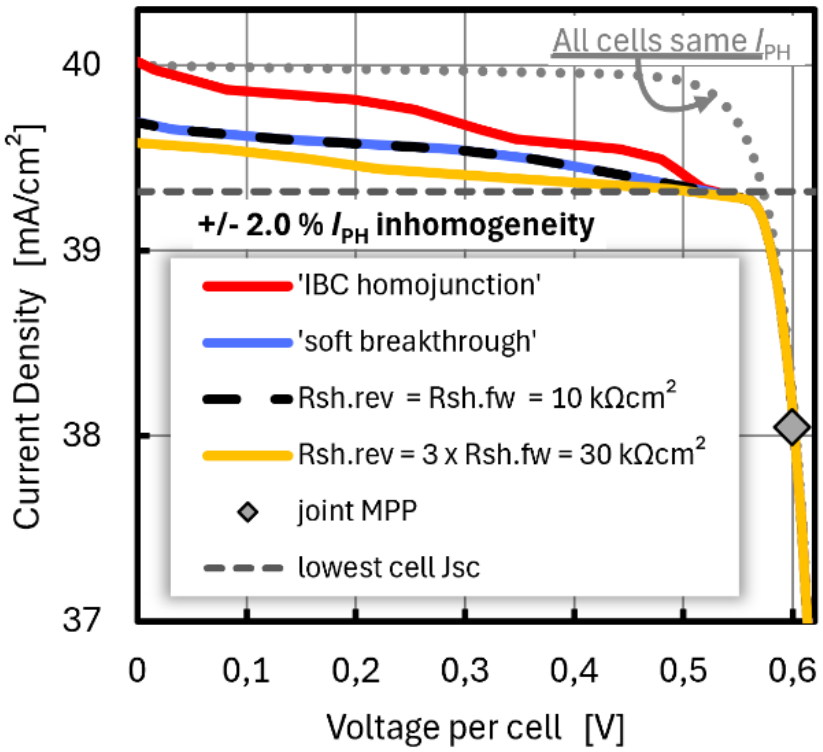

Figure 9: Zoom into upper current range of 1-Sun I -V curves with +/- 2.0% photogeneration inhomogeneity, plotted for the four cases of different cell reverse bias characteristics in Fig. 6. (Also shown for comparison: I -V curve with homogeneous I_{PH} distribution, grey dotted line.) Despite different $R_{\mathrm{Sh.Slope}}$ values, all I -V curves share the same MPP.

The reason for all curves sharing the same MPP is that the maximum power current of the module is still notably lower than the lowest photogeneration current in the inhomogeneity distribution. Consequently, even the solar cell with the smallest I_{SC} in the module circuit does not block the current at MPP, and this cell with the lowest I_{SC} can still produce a significant fraction of its maximum power at the global module maximum power current I_{MP}.

Fig. 9 shows that the black dashed line I -V curve [i.e. the module of case 3 in Fig. 6] is indistinguishable from the blue line I -V curve [case 2 in Fig. 6]. The reverse characteristics of the "case 3 cells" is defined by extending their forward shunt resistance R_{Sh} =10 kcm^2 to the reverse bias direction, while the "case 2 cells", that form the blue I -V curve in Fig. 9, have additionally to a reverse shunt resistance of 10

kcm2 also a breakdown characteristic that increases current conduction superlinearly in reverse voltage direction. However, despite their differences for larger reverse bias voltages, both reverse bias characteristics are nevertheless virtually identical for the first 4 volts, from zero to -4 V. Since the moderate current inhomogeneities considered here do not cause cells in these two module types to exceed reverse bias voltages of -4V, their I -V curves in Fig. 9 do not differ.

In order to highlight the 'near-irrelevance' of the apparent shunt $R_{\text{Sh.Slope}}$ for module's power production, Fig. 10 plots the module efficiency as a function of illumination intensity for the two most extremely different inhomogeneity cases of this study: The 'IBC homojunction' case at an inhomogeneity level of +/- 0.4%, and the case with the highest reverse bias shunt resistance $R_{\text{Sh.rev}} = 30$ kcm2. at an inhomogeneity level of +/- 2.0%. We can see that the efficiency differences between these two cases is marginal and reaches only a maximum deviation of $0.026\%_{\text{abs}}$, i.e. $0.11\%_{\text{rel}}$, at the at highest illumination intensity.

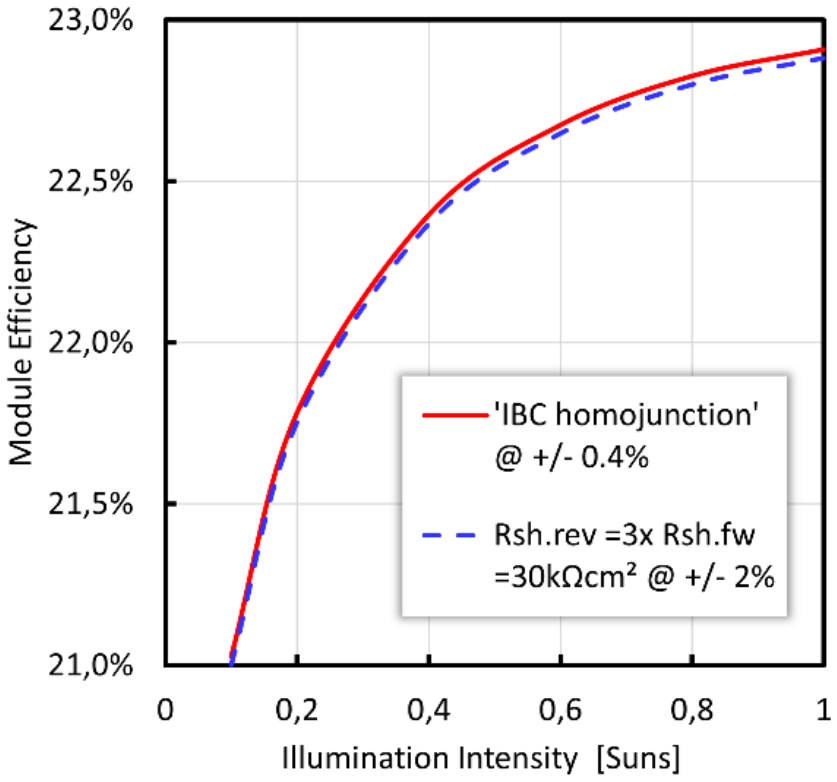

Figure 10: Efficiency as a function of illumination intensity for the two most extremely different cases of reverse bias characteristics (see Fig. 6), paired with the two most different photogeneration inhomogeneities used in this study (+/- 0.4% and +/- 2.0%). Average photogeneration is in all cases 40 mA/cm**²**. The efficiency is calculated assuming that inhomogeneity is exclusively due to illumination, and hence both modules receive identical average illumination intensity for all cases from 0.1 Sun to 1 Sun.

The modules of all four different I -V curves in Fig. 9 received the same average photogeneration current density 40 mA/cm**²**, but produced different short-circuit currents I_{SC}. We therefore explore in Fig. 11 how the I_{SC} varies as a function of illumination inhomogeneity and intensity for modules with different cell reverse bias characteristics.

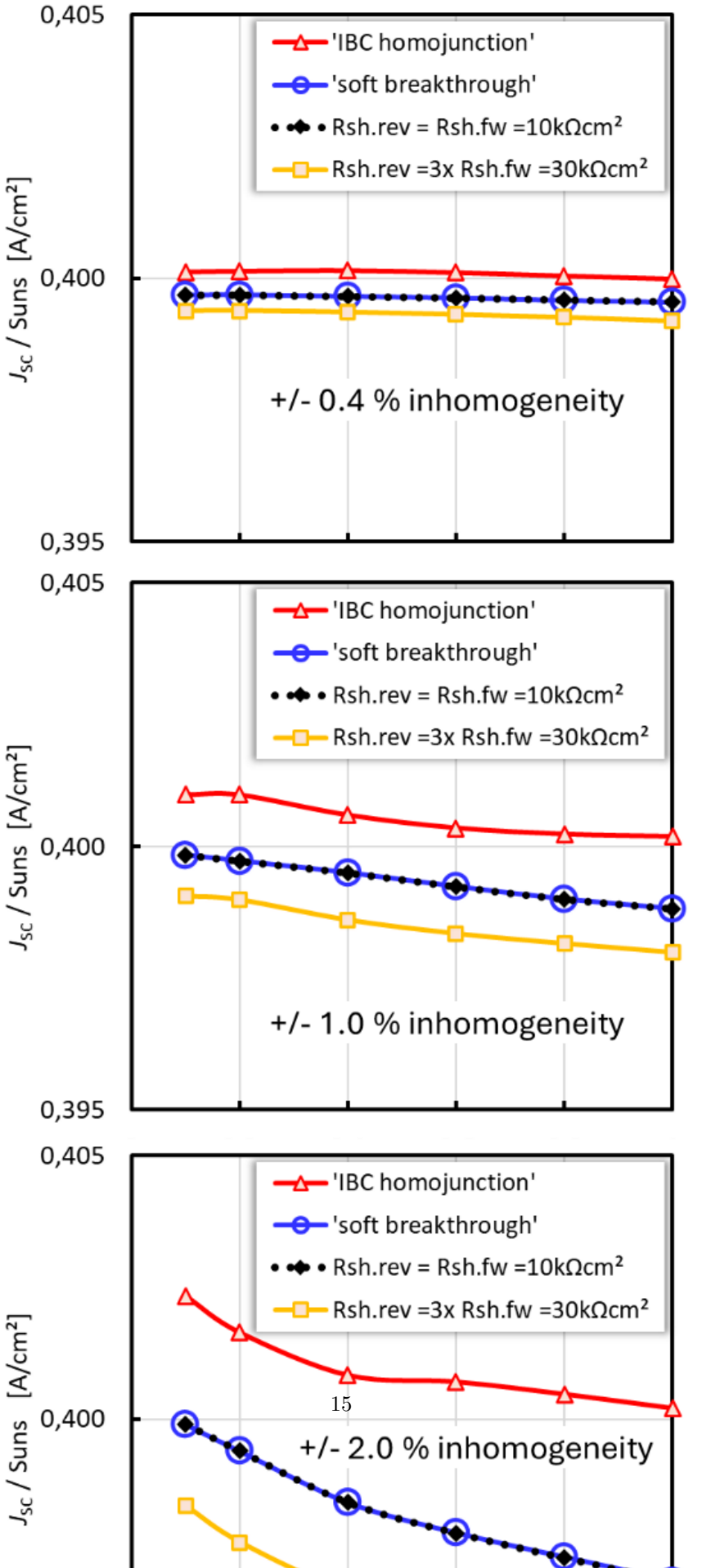

Figure 11: Short-circuit current density of the modules, normalized by the illumination intensity, plotted as a function of illumination intensity. For increasing inhomogeneity, the quality of the proportionality between short-circuit current $I_{SC}$and illumination intensity is reduced, even though every single cell in the module circuit features liner I_{PH}-Suns relation and hence a near-perfect proportionality(linearity) of cellI_{SC} and illumination intensity.

We can see from the variation of the ratioI_{SC}/Suns in Fig. 11 that theI_{SC} of modules is not linear with illumination intensity if the photogeneration I_{PH} of the individual cells is not homogeneous across the module. This is an interesting observation and potentially of importance in situations where one may be tempted to use the module I_{SC} as a measure for the average photogeneration, such as when analyzing soiling of modules in the field. In such cases it is actually better to observe the maximum power, or the current at the maximum power point. This is demonstrated in Fig. 9, where all curves shared the same MMP, which is also shared by the grey dotted I -V curve that features in all cells the average photogeneration of the inhomogeneous distribution of the other curves.

The non-linearity of I_{SC} with (average) intensity of the illumination, as explored in Fig. 11, does not mean a model for power production of PV systems would need to take into account such non-linearity. Instead, Fig. 9 has shown that the MPP, which lies for reasonable non-degenerate cell photogeneration distributions well outside the voltage range affected by cell I_{SC}current mismatch, can be well described with using the average photogeneration. The average photogeneration I_{PH}scales well with the illumination intensity. Hence, the results presented here rather underline that an equivalent circuit model (e.g. 1-Diode model) for PV system power production simulation can and should scale the photogeneration I_{PH} linearly with illumination intensity. The challenge lies only in determining a suitable 1-Diode parameterization of the module I -V curve, including the average cell I_{PH} ($\approx I_{SC}$) for use in the 1-Diode model parameterization of the module.

4 CONCLUSIONS

We have shown how an apparent shunt emerges in a module$I$ -V curve from combining cells with different photogeneration in the module circuit. Since the difference of photogeneration scales with illumination intensity, this apparent shunt in the module I -V curve scales with illumination intensity. However, this effect is not at all an actual shunt conductance and appears only when applying a method for shunt analysis that is only appropriate for single cells: The slope of the module$I$ -V curve in the quasi-linear range fromI_{SC} towards larger voltages is not a good indication a shunt conductance in the module. When the cells in the module have different photogeneration, which can be caused by illumination inhomogeneities or by cell production variations, this slope is strongly influenced by current mismatch effects.

We show that this mismatch induced slope in the quasi-linear range of the I -V curve has no influence on the I -V curve near MPP. However, interpreting this slope as a shunt (or rather: "pseudo shunt") and using this value as shunt conductance in an equivalent circuit model for the module, such as the 1-Diode model, does affect the MPP. Consequently, the slope-derived pseudo shunt value should not be used as shunt conductance in equivalent circuit models for representing the module power production performance.

5 REFERENCES

[1] W. De Soto, S.A. Klein and W.A. Beckman, "Improvement and validation of a model for photovoltaic array performance", Solar Energy 80 (2006), p. 78-88.

[2] A. Mermoud and T. Lejeune, "Performance assessment of a simulation model for PV modules of any available technology", 25th EU-PVSEC (2010), Valencia, Spain.

[3] G.E. Bunea, K.E. Wilson, Y. Meydbray, M.P. Campbell and D.M. De Ceuster, "Low light performance of mono-crystalline silicon solar cells", IEEE 4th WC-PEC, 2006, pp. 1312-1314..

[4] S. J. Robinson, A. G. Aberle, and M.A. Green, "Departures from the principle of superposition in silicon solar cells", Journal of Applied Physics 76, (1994), p. 7920-7930.

[5] O. Breitenstein, "An alternative one-diode model for illuminated solar cells", Energy Procedia 55 (2014) p. 30 – 37.

[6] K. Ramspeck, C. Böhmer, and M. Meixner, "Measurement Uncertainty Analysis for Large Area High-Efficiency Modules", 40$^{\text{th}}$ European Photovoltaic Solar Energy Conference, (2023), p. 020213-001 - 020213-005.

[7] N.-P. Harder, and J. Cano Carcia, "TOPCon module characterization at different temperatures and intensities: Revision of shunt parameterization by De Soto and PVsyst", 52$^{\text{nd}}$IEEE Photovoltaics Specialists Conference (2024), proceedings in print.

[8] C.E. Clement, J. Prakash Singh, E. Birgersson, Y. Wang, and Y. Sheng Khoo, "Illumination Dependence of Reverse Leakage Current in Silicon Solar Cells", IEEE Journal of Photovoltaics, Vol. 11(5), 2021, p. 1285.